

# Polarization Diversity for Detecting Targets in Inhomogeneous Clutter

*Martin Hurtado and Arye Nehorai*

Department of Electrical and Systems Engineering  
Washington University in St. Louis  
One Brookings Drive, St. Louis, MO 63130  
Email: {mhurta3, nehorai}@ese.wustl.edu

**Abstract**—Polarization diversity has proved to be a useful tool for radar detection, especially when discrimination by Doppler effect is not possible. In this paper, we address the problem of improving the performance of polarimetric detectors for targets in heavy inhomogeneous clutter. First, we develop a polarimetric detection test that is robust to inhomogeneous clutter. We run this polarimetric test against synthetic and real data to assess its performance in comparison with existing polarimetric detectors. Then, we propose a polarimetric waveform-design algorithm to further improve the target-detection performance. A numerical analysis is presented to demonstrate the potential performance improvement that can be achieved with this algorithm.

## I. INTRODUCTION

The detection of static or slowly moving targets in heavy-clutter environments is considered a challenging problem, mainly because it is not possible to discriminate the target from the clutter using the Doppler effect. Polarization diversity provides additional information that enhances the detection of targets, particularly under the conditions described above. Detection performance could be further improved if the polarization of the transmitted signal were optimally selected to match the target polarimetric aspects.

Earlier work in the field of polarimetric detection has addressed the design of detectors under the assumption that training data is available [1]-[3]. The performance of these detectors can be severely degraded in the presence of inhomogeneous and non-stationary clutter. To overcome this problem, the application of compound-Gaussian distributions for modeling the global behavior of nonhomogeneous clutter has been proposed. However, the use of non-Gaussian models increases the difficulty of developing efficient detection algorithms. For instance, the detection statistic derived from the scheme presented in [4] has a closed-form expression only for the special case of two polarimetric channels, and the detector proposed in [5] does not support the constant false-alarm rate (CFAR) property with respect to the clutter covariance.

In this paper, we first develop a polarimetric detector whose decision-making capability is based only on the data collected from the range cell under test, without resorting to secondary data or prior knowledge of the target and clutter. This feature makes it robust against inhomogeneous and

non-stationary clutter. Later in this paper, we address the problem of waveform design by presenting an algorithm for selecting the waveform polarization. The developed test statistic has a closed-form expression that incorporates information about the transmitted signal polarization. Hence, analysis of detection performance is used to select the next transmission polarization, which improves the target detection.

## II. POLARIMETRIC RADAR MODEL

We consider a mono-static radar capable of transmitting waveforms with any arbitrary polarization on a pulse-by-pulse basis. In addition, we assume that the radar system illuminates a point target. The recorded data from the range cell under test consist not only of the target echoes but also of the undesired reflections from the target environment (clutter).

### A. Polarimetric Data

The output of a diversely polarized array of  $Q$  sensors receiving the echoes from the cell under test can be expressed as

$$\mathbf{y}(t) = B (S^t + S^c) \boldsymbol{\xi}(t) + \mathbf{e}(t), \quad t = 1, \dots, N, \quad (1)$$

where

- The  $Q \times 1$  vector  $\mathbf{y}(t)$  is the complex envelope of the measurements.
- The  $Q \times 2$  matrix  $B$  is the response of the diversely polarized sensor array. If the receiver array is a vector sensor [6], the array response is given by

$$B = \begin{bmatrix} -\sin \phi & -\cos \phi \sin \psi \\ \cos \phi & -\sin \phi \sin \psi \\ 0 & \cos \psi \\ -\cos \phi \sin \psi & \sin \phi \\ -\sin \phi \sin \psi & -\cos \phi \\ \cos \psi & 0 \end{bmatrix}, \quad (2)$$

where  $\phi$  and  $\psi$  are the azimuth and elevation angles of the cell under test, respectively. For a conventional polarized radar measuring the horizontal and vertical components of the electric field and assuming these two sensors are orthogonal to the direction that points toward the cell under test, the array response matrix is  $B = I_2$ .

- The complex scattering matrix  $S$  represents the polarization change of the transmitted signal upon its reflection on the target or clutter:

$$S = \begin{bmatrix} s_{11} & s_{12} \\ s_{21} & s_{22} \end{bmatrix}, \quad (3)$$

where the variables  $s_{11}$  and  $s_{22}$  are co-polar scattering coefficients and  $s_{12}$  and  $s_{21}$  are cross-polar coefficients. For the mono-static radar case,  $s_{12} = s_{21}$ . The superscripts  $t$  and  $c$  refer to the target and clutter.

- The vector  $\xi(t)$  is the narrowband transmitted polarized signal which can be represented by

$$\xi(t) = \begin{bmatrix} \xi_1 \\ \xi_2 \end{bmatrix} s(t) = \begin{bmatrix} \cos \alpha & \sin \alpha \\ -\sin \alpha & \cos \alpha \end{bmatrix} \begin{bmatrix} \cos \beta \\ j \sin \beta \end{bmatrix} s(t), \quad (4)$$

where  $\xi_1$  and  $\xi_2$  are the signal components on the polarization basis of the transmitter,  $\alpha$  and  $\beta$  are the orientation and ellipticity angles, respectively, and  $s(t)$  is the complex envelope of the transmitted signal.

- The vector  $e(t)$  represents the thermal noise.

Equation (1) can be written as

$$\mathbf{y}(t) = s(t)B\bar{\xi}(\boldsymbol{\mu} + \mathbf{x}) + e(t), \quad (5)$$

where the scattering coefficient vectors of the target and clutter are  $\boldsymbol{\mu} = [s_{hh}^t, s_{vv}^t, s_{hv}^t]^T$  and  $\mathbf{x} = [s_{hh}^c, s_{vv}^c, s_{hv}^c]^T$ , respectively, which have dimension  $P = 3$ . The polarization matrix  $\bar{\xi}$  is

$$\bar{\xi} = \begin{bmatrix} \xi_1 & 0 & \xi_2 \\ 0 & \xi_2 & \xi_1 \end{bmatrix}. \quad (6)$$

The time samples can be stacked in one vector of dimension  $NQ \times 1$ :

$$\mathbf{y} = (\mathbf{s} \otimes B\bar{\xi})(\boldsymbol{\mu} + \mathbf{x}) + \mathbf{e}, \quad (7)$$

where  $\mathbf{s} = [s(1), \dots, s(N)]^T$  and  $\otimes$  is the Kronecker product. Piling together the data corresponding to pulses of different polarization yields

$$\mathbf{y} = A\boldsymbol{\mu} + A\mathbf{x} + \mathbf{e}, \quad (8)$$

where  $A$  is a  $M \times P$  ( $M = KNQ$ ) complex matrix that represents the system response:

$$A = \begin{bmatrix} \mathbf{s} \otimes B\bar{\xi}_1 \\ \vdots \\ \mathbf{s} \otimes B\bar{\xi}_K \end{bmatrix}, \quad (9)$$

and  $\bar{\xi}_k$  is the polarization matrix of each diversely polarized pulse ( $k = 1, \dots, K$ ).

### B. Statistical Model

We assume that the target is a small man-made object; hence,  $\boldsymbol{\mu}$  is a deterministic vector. On the other hand, the clutter in the range cell under test can be considered as a large collection of point scatterers producing incoherent reflections of the radar signal. Then,  $\mathbf{x}$  is a zero-mean complex Gaussian random vector with covariance matrix  $\Sigma$ . The noise  $\mathbf{e}$  is a zero-mean complex Gaussian random vector with covariance matrix  $\sigma I_M$ , where  $I_M$  is the  $M \times M$  identity matrix. In

addition, we assume that the clutter reflections and the thermal noise are statistically independent.

The radar dwell consists of a series of pulses that can be seen as ‘‘snapshots’’ of the range cell under test. If the pulse duration is short with respect to the dynamic of the target and its environment, it is reasonable to assume that their scattering coefficients are constant during each pulse. However, from pulse to pulse, we consider the clutter scattering coefficients as independent realizations of the same random process. Then, the distribution of each snapshot is

$$\mathbf{y}_d \sim \mathcal{CN}(A\boldsymbol{\mu}, A\Sigma A^H + \sigma I_M), \quad d = 1, \dots, D, \quad (10)$$

where  $D$  is the total number of snapshots or pulses in the radar dwell and  $^H$  denotes the conjugate transpose operator.

### C. Known and Unknown Model Parameters

We assume the system response matrix  $A$  is known, since we consider that the receiver antenna array has been calibrated. In addition, we assume that the power of the thermal noise  $\sigma$  is known, because it can be easily estimated from the recorded data when no signal has been transmitted. However, we suppose that we have no prior knowledge about the target and the clutter, nor do we count on a secondary data set for estimating the statistical properties of the clutter. Hence, the vector  $\boldsymbol{\mu}$  and the matrix  $\Sigma$  are the unknown parameters of the statistical data model (10).

## III. DETECTION TEST

We aim to decide whether a target is present or not in the range cell under test, based on the recorded data. Then, the decision problem consists of choosing between two possible hypotheses: the null hypothesis  $\mathcal{H}_0$  (target-free hypothesis) or the alternative hypothesis  $\mathcal{H}_1$  (target-present hypothesis)

$$\begin{cases} \mathcal{H}_0 : \boldsymbol{\mu} = 0, \Sigma \\ \mathcal{H}_1 : \boldsymbol{\mu} \neq 0, \Sigma \end{cases} \quad (11)$$

where the matrix  $\Sigma$  is considered as a nuisance parameter. Next, we derive the generalized likelihood ratio (GLR) test [7] and study its performance. We omit derivation details in this paper due to space limitation; refer to [10] for an extended version of this paper.

### A. GLR Test

The logarithmic GLR test decides  $\mathcal{H}_1$  if

$$\ln L_{\text{GLR}} = \ln f_1(\mathbf{y}_1, \dots, \mathbf{y}_D; \hat{\boldsymbol{\mu}}_1, \hat{\Sigma}_1) - \ln f_0(\mathbf{y}_1, \dots, \mathbf{y}_D; \hat{\Sigma}_0) > \gamma, \quad (12)$$

where  $f_0$  and  $f_1$  are the likelihood functions under  $\mathcal{H}_0$  and  $\mathcal{H}_1$ ,  $\hat{\Sigma}_0$  and  $\hat{\Sigma}_1$  are the MLEs of  $\Sigma$  under  $\mathcal{H}_0$  and  $\mathcal{H}_1$ ,  $\hat{\boldsymbol{\mu}}_1$  is the MLE of  $\boldsymbol{\mu}$  under  $\mathcal{H}_1$ , and  $\gamma$  is the detection threshold. For simplicity of notation we will omit references to the data in the arguments of the functions  $f_0$  and  $f_1$  in the rest of the paper.

We start the derivation of the GLR test by determining the likelihood functions and MLEs of the unknown parameters. Under hypothesis  $\mathcal{H}_0$ , it is assumed that  $\boldsymbol{\mu} = 0$ ; then

$$\ln f_0(\Sigma) = -D [M \ln \pi + \ln |C| + \text{tr}(C^{-1}S_0)], \quad (13)$$

where  $C = A\Sigma A^H + \sigma I_M$  is the theoretical covariance matrix of the data, defined in (10), and  $S_0$  is the sample covariance matrix

$$S_0 = \frac{1}{D} \sum_{d=1}^D \mathbf{y}_d \mathbf{y}_d^H. \quad (14)$$

The MLE of  $\Sigma$  is

$$\hat{\Sigma}_0 = A^+ S_0 A^{+H} - \sigma (A^H A)^{-1}, \quad (15)$$

where  $A^+ = (A^H A)^{-1} A^H$  is the generalized matrix inverse. Under hypothesis  $\mathcal{H}_1$ , the likelihood function is

$$\ln f_1(\boldsymbol{\mu}, \Sigma) = -D \left[ M \ln \pi + \ln |C| + \text{tr}(C^{-1} \tilde{C}_1) \right], \quad (16)$$

where

$$\tilde{C}_1 = \frac{1}{D} \sum_{d=1}^D (\mathbf{y}_d - A\boldsymbol{\mu})(\mathbf{y}_d - A\boldsymbol{\mu})^H. \quad (17)$$

The MLE of the unknown parameters are

$$\hat{\boldsymbol{\mu}}_1 = A^+ \bar{\mathbf{y}}, \quad (18)$$

$$\hat{\Sigma}_1 = A^+ S_1 A^{+H} - \sigma (A^H A)^{-1}, \quad (19)$$

where  $\bar{\mathbf{y}}$  is the sample mean vector

$$\bar{\mathbf{y}} = \frac{1}{D} \sum_{d=1}^D \mathbf{y}_d, \quad (20)$$

and  $S_1$  is the sample covariance matrix

$$S_1 = \frac{1}{D} \sum_{d=1}^D (\mathbf{y}_d - \bar{\mathbf{y}})(\mathbf{y}_d - \bar{\mathbf{y}})^H. \quad (21)$$

Then, substituting the MLEs and likelihood functions in (12), and after some mathematical simplification, the GLR test can be written as

$$L_{\text{GLR}} = \left[ 1 + \bar{\mathbf{y}}^H A (A^H S_1 A)^{-1} A^H \bar{\mathbf{y}} \right]^D. \quad (22)$$

Since (22) is a monotonically increasing function of the second term inside the brackets, an equivalent detection test statistic can be defined as

$$T_{\text{GLR}} = \bar{\mathbf{y}}^H A (A^H S_1 A)^{-1} A^H \bar{\mathbf{y}}. \quad (23)$$

### B. Detection Performance

Applying Corollary 5.2.1 from [8], it is straightforward to verify that the detection statistic (23) is distributed as follows

$$T_{\text{GLR}} \frac{D-P}{P} \sim \begin{cases} \mathcal{F}_{2P, 2(D-P)} & \text{under } \mathcal{H}_0 \\ \mathcal{F}'_{2P, 2(D-P)}(\lambda) & \text{under } \mathcal{H}_1 \end{cases} \quad (24)$$

where  $\mathcal{F}_{\nu_1, \nu_2}$  denotes an  $F$  distribution with  $\nu_1$  and  $\nu_2$  degrees of freedom, and  $\mathcal{F}'_{\nu_1, \nu_2}(\lambda)$  denotes a non-central  $F$  distribution with  $\nu_1$  and  $\nu_2$  degrees of freedom and non-centrality parameter  $\lambda$ . The non-centrality parameter is given by

$$\lambda = 2D\boldsymbol{\mu}^H \left[ \Sigma + \sigma (A^H A)^{-1} \right]^{-1} \boldsymbol{\mu}. \quad (25)$$

Thus, the detection performance becomes

$$\begin{aligned} P_{\text{FA}} &= Q_{\mathcal{F}_{2P, 2(D-P)}}(\gamma') \\ P_{\text{D}} &= Q_{\mathcal{F}'_{2P, 2(D-P)}(\lambda)}(\gamma'), \end{aligned} \quad (26)$$

where  $Q$  is the right-tail probability function [7, Chap. 2] and  $\gamma'$  is the detection threshold for the required probability of false alarm. In particular, note that the expression for  $P_{\text{FA}}$  does not depend on the covariance of clutter and thermal noise, nor on the transmitted signal; hence, equation (23) is a CFAR test.

### C. Detector Performance in Inhomogeneous Clutter

A significant characteristic of the detector presented in this paper is that the test statistic (23) is computed using only data from the cell under test. No assumption is required about the range homogeneity of the clutter. Thus, the detector is robust against spatially fluctuating clutter.

To support this assertion, the  $P_{\text{FA}}$  is computed using  $5 \cdot 10^5$  runs of Monte Carlo simulations in the presence of inhomogeneous clutter. The clutter echoes are assumed to follow a compound-Gaussian distribution with covariance matrix  $\tau\Sigma$ . The texture  $\tau$  has a generalized Gamma probability density function [4]:

$$p(\tau) = \frac{1}{\Gamma(\nu)} \left( \frac{\nu}{\delta} \right)^\nu \tau^{\nu-1} \exp\left(-\frac{\nu}{\delta} \tau\right), \quad (27)$$

where  $\nu$  is the order parameter and  $\delta$  is the average power. Note that  $\nu = \infty$  corresponds to clutter echoes with Gaussian distribution, but when  $\nu$  decreases, they deviate from Gaussian. Additional information about the simulation setup is as follows. The transmitted signals are rectangular pulses, which are transmitted in a sequence of alternating vertical (V) and horizontal (H) polarization ( $K = 2$ ). The radar dwell consists of 10 repetitions of this polarimetric sequence ( $D = 10$ ). On the receiver side, samples of the V and H electric field are recorded ( $Q = 2$ ) at a rate of one sample per pulse ( $N = 1$ ). Since the simulations are intended to compute the  $P_{\text{FA}}$ , no target is considered. The average power of the texture is  $\delta = 50$  and the covariance of the speckle component is  $\Sigma = I_3$ .

For comparison purposes, we also compute the performance of two other polarimetric detectors that use secondary data:

- Polarization-space-time GLR (PST-GLR): This detector was derived under the assumption of homogeneous Gaussian clutter [1].
- Texture free GLR (TF-GLR): This detector was formulated assuming that the clutter follows a compound-Gaussian distribution [4].

In Fig. 1, the  $P_{\text{FA}}$  of our detection test  $T_{\text{GLR}}$ , as well as of the PST-GLR and TF-GLR tests, is plotted as a function of the order parameter of the clutter texture distribution. For the latter two tests, we consider 80 adjacent range cells for generating the secondary data. We observe that the performance of our detector  $T_{\text{GLR}}$  and the TF-GLR test remains constant at the designed false-alarm rate. However, there is a discrepancy between the design and the actual clutter that increases the probability of false alarm for the PST-GLR test as the clutter process departs from being Gaussian.

### D. Detector Performance Using Real Data

To evaluate the performance of the polarimetric detectors in a real application situation, we use data collected at the

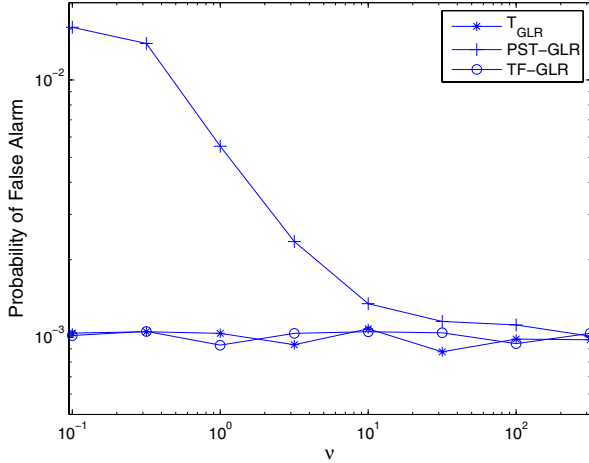


Fig. 1. Probability of false alarm as a function of the order parameter  $\nu$  of the clutter texture distribution.

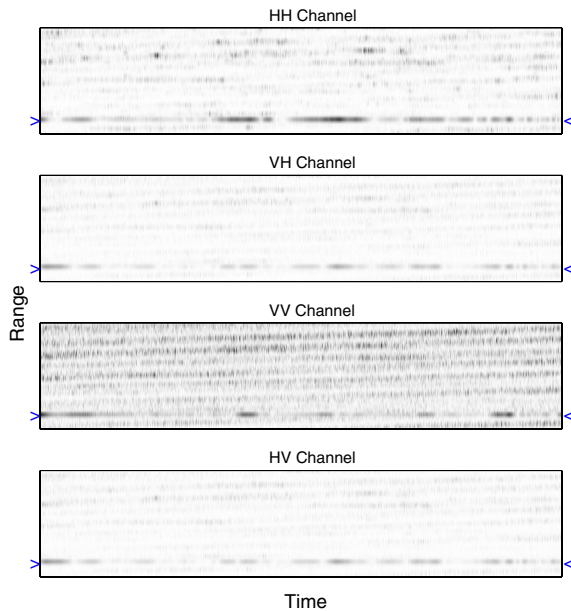


Fig. 2. Magnitude in range and time domain of the IPIX radar dataset *stare1*, collected on November 11, 1993. The target location is indicated by the markers “>” and “<”.

Osborne Head Gunnery Range (OHGR), Dartmouth, Nova Scotia, Canada, with the McMaster University IPIX radar [9]. Specifically, we use the data recorded on November 11, 1993. Fig. 2 shows the magnitude of the echoes from a small target in inhomogeneous sea clutter of the four polarimetric channels: HH, VH, VV, and HV.

Fig. 3 shows detection maps for the  $T_{\text{GLR}}$ , PST-GLR and TF-GLR tests, setting the threshold for  $P_{\text{FA}} = 10^{-3}$ . For the latter two tests, a guard region of two range cells on either side of the cell under test is used to avoid the leakage of the target energy into the secondary data. We observe that our detection test finds the true position of the target with only a few false detections despite the strong clutter echoes,

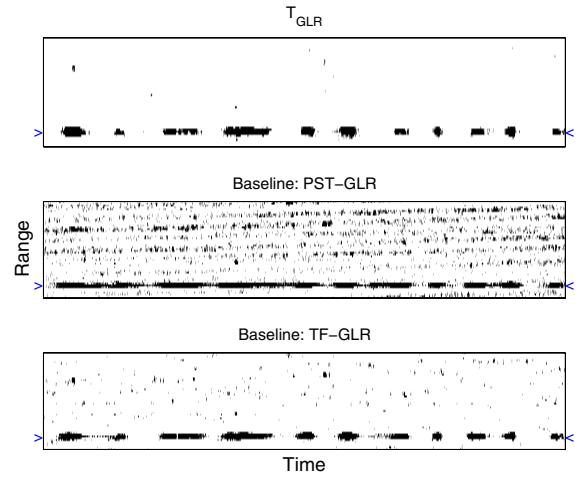


Fig. 3. Detection map in range and time domain for the IPIX radar dataset *stare1*, collected on November 11, 1993. Black pixels indicate that the detection statistic is larger than the threshold. The target location is indicated by the markers “>” and “<”.

which can be appreciated from Fig. 2. On the other hand, the PST-GLR has high false-alarm rate due to the presence of inhomogeneous clutter, as was predicted in the previous subsection. The TF-GLR test greatly reduces the false-alarm rate with respect to the PST-GLR test; however, it still remains considerably high.

We acknowledge that comparing the TF-GLR test with the other two is not strictly fair, since the closed form of this test was developed for only two polarimetric channels (we have used HH and VV for the previous results). Our goal is not to extend the work in [4] but to show that polarimetric detection tests using secondary data may have larger false false-alarm than their designed value, in the case of inhomogeneous clutter.

#### IV. TARGET DETECTION OPTIMIZATION

We aim at improving target detection by optimizing the design of our system. In the previous section, we have shown that the target probability of detection depends on the system characteristics through the non-centrality parameter  $\lambda$ , which in turn depends on the system response  $A$ . We recall that matrix  $A$  carries the information of the transmitted waveform and the receiver sensor array. Our optimization approach consists of designing the matrix  $A$  in order to maximize the parameter  $\lambda$ , and consequently the probability of detection.

In order to find the value of the matrix  $A$  that maximizes the parameter  $\lambda$ , we rewrite Equation (25) as

$$\frac{\lambda}{2D} = \boldsymbol{\mu}^H \boldsymbol{\Sigma}^{-1} \boldsymbol{\mu} - \boldsymbol{\mu}^H \left( \boldsymbol{\Sigma} + \frac{\boldsymbol{\Sigma} A^H A \boldsymbol{\Sigma}}{\sigma} \right)^{-1} \boldsymbol{\mu}. \quad (28)$$

Maximizing  $\lambda$ , given  $\boldsymbol{\mu}$  and  $\boldsymbol{\Sigma}$ , is equivalent to minimizing the second term of (28). Assuming that  $\boldsymbol{\eta}$  is a vector whose entries are the parameters of the transmit waveforms, the system response matrix is parameterized as  $A = A(\boldsymbol{\eta})$ . Thus,

to improve detection, we seek

$$\hat{\boldsymbol{\eta}} = \arg \min_{\boldsymbol{\eta}} \left\{ \boldsymbol{\mu}^H \left[ \Sigma + \frac{\Sigma A^H(\boldsymbol{\eta}) A(\boldsymbol{\eta}) \Sigma}{\sigma} \right]^{-1} \boldsymbol{\mu} \right\}. \quad (29)$$

We first solve the product  $A^H A$  using the system response matrix given by (9), obtaining

$$A^H A = c \mathcal{P}_s \sum_{k=1}^K \bar{\boldsymbol{\xi}}_k^H \bar{\boldsymbol{\xi}}_k, \quad (30)$$

where the value of the coefficient  $c$  depends of the receiver sensor array, and  $\mathcal{P}_s$  is the transmit signal energy:

$$\mathcal{P}_s = \sum_{t=1}^N |s(t)|^2. \quad (31)$$

The constant  $c$  for a conventional V/H sensor array is  $c = 1$ ; and for the electromagnetic vector sensor is  $c = 2$ . Thus, the performance of our polarimetric detector does not depend on the pulse envelope of the waveform but rather on the polarization parameters  $\boldsymbol{\eta} = [\alpha_1, \beta_1, \dots, \alpha_K, \beta_K]$ .

We mention here that in a real application the true values of  $\boldsymbol{\mu}$  and  $\Sigma$  are not known. Instead, their estimates  $\hat{\boldsymbol{\mu}}_1$  and  $\hat{\Sigma}_1$  should be used. Nevertheless, solving Equation (29) with the true target and clutter values provides an upper bound of the detection improvement.

#### A. Simulation Example

In order to study the detection improvement by optimally selecting the signal polarization, we design a simple problem. We assume a system in which the first pulse is vertically polarized and the second can be of any arbitrary polarization. When the second pulse is horizontal, this system corresponds to a conventional polarimetric radar. Fig. 4 shows the average detection performance of 1000 cases where parameters  $\boldsymbol{\mu}$  and  $\Sigma$  were randomly selected. The figure shows the average performance of the conventional system (the second pulse has fixed H polarization) in addition to the results obtained when the polarization is optimally selected to satisfy Equation (29) and when the worst possible polarization is selected. We observe that the performance of the conventional system is somewhere in between the optimal and worst polarization. Specifically, the optimal polarization shows, for  $P_D = 0.5$ , a reduction of 1.5dB of target-to-clutter ratio with respect to the conventional system and 3.8dB with respect to the worst polarization.

#### V. CONCLUSIONS

In this paper, we addressed the problem of detecting small and slowly moving targets in heavy inhomogeneous clutter by exploiting polarization diversity. To improve the detection performance, we first developed a new polarimetric detector that is robust against space and time variations of the clutter. The proposed detector decides the presence of a target based only on the data recorded from the cell under test, without requiring secondary data or prior knowledge about the clutter. We tested this detector with synthetic and real data, and it

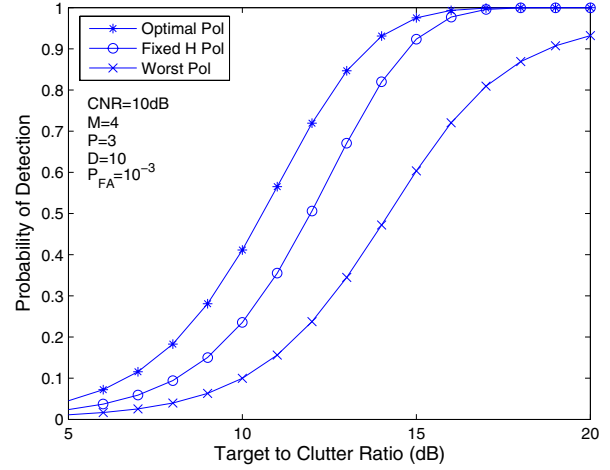


Fig. 4. Detection performance of the GLR test statistic  $T_{\text{GLR}}$  as a function of the target-to-clutter ratio, for  $P_{\text{FA}} = 10^{-3}$ .

demonstrated a significant performance improvement with respect to other polarimetric detectors. An additional advantage of our detection algorithm is that it is computationally less intense because it does not require recording and processing of training data. Furthermore, we proposed an adaptation rule for designing the transmit polarization by maximizing the non-centrality parameter of the detector distribution in order to improve the target-detection performance. We showed that the detection performance depends on the signal polarization, but no on the pulse envelope. A numerical experiment was presented to demonstrate the performance improvement that could be obtained from the adaptation rule.

#### REFERENCES

- [1] H. Park, J. Li, and H. Wang, "Polarization-space-time domain generalized likelihood ratio detection of radar targets," *Signal Processing*, Vol. 41, pp. 153-164, Jan. 1995.
- [2] D. Pastina, P. Lombardo, and T. Bucciarelli, "Adaptive polarimetric target detection with coherent radar. Part I: Detection against Gaussian background," *IEEE Trans. Aerosp. Electr. Syst.*, Vol. 37, pp. 1194-1206, Oct. 2001.
- [3] A. De Maio and G. Ricci, "A polarimetric adaptive matched filter," *Signal Processing*, Vol. 81, pp. 2583-2589, Dec. 2001.
- [4] P. Lombardo, D. Pastina, and T. Bucciarelli, "Adaptive polarimetric target detection with coherent radar. Part II: Detection against non-Gaussian background," *IEEE Trans. Aerosp. Electr. Syst.*, Vol. 37, pp. 1207-1220, Oct. 2001.
- [5] A. De Maio and G. Alfano, "Polarimetric adaptive detection in non-Gaussian noise," *Signal Processing*, Vol. 83, pp. 297-306, Feb. 2003.
- [6] A. Nehorai and E. Paldi, "Vector-sensor array processing for electromagnetic source localization," *IEEE Trans. Signal Process.*, Vol. 42, pp. 376-398, Feb. 1994.
- [7] S. M. Kay, *Fundamentals of Statistical Signal Processing: Detection Theory*, Englewood Cliffs, NJ: Prentice Hall, 1993.
- [8] T. W. Anderson, *An Introduction to Multivariate Statistical Analysis*, 3rd Ed., Hoboken, NJ: John Wiley & Sons, 2003.
- [9] S. Haykin, C. Krasnor, T. J. Nohara, B. W. Currie, and D. Hamburger, "A coherent dual-polarized radar for studying the ocean environment," *IEEE Trans. Geosci. Remote Sensing*, Vol. 29, pp. 189-191, Jan. 1991.
- [10] M. Hurtado and A. Nehorai, "Polarimetric detection of targets in heavy inhomogeneous clutter," submitted to *IEEE Trans. Signal Process.*